Cell, Vol. 108, 705–715, March 8, 2002, Copyright ©2002 by Cell Press

A TRP Channel that Senses Cold Stimuli and Menthol

Andrea M. Peier,[1] Aziz Moqrich,[2] Anne C. Hergarden,[1] Alison J. Reeve,[3] David A. Andersson,[3] Gina M. Story,[2] Taryn J. Earley,[2] Ilaria Dragoni,[3] Peter McIntyre,[3] Stuart Bevan,[3] and Ardem Patapoutian[1,2,4]

[1]Genomics Institute of the Novartis Research Foundation
San Diego, California 92121
[2]Department of Cell Biology
The Scripps Research Institute
La Jolla, California 92037
[3]Novartis Institute for Medical Sciences
London WC1E 6BN
United Kingdom

Summary

A distinct subset of sensory neurons are thought to directly sense changes in thermal energy through their termini in the skin. Very little is known about the molecules that mediate thermoreception by these neurons. Vanilloid Receptor 1 (VR1), a member of the TRP family of channels, is activated by noxious heat. Here we describe the cloning and characterization of TRPM8, a distant relative of VR1. TRPM8 is specifically expressed in a subset of pain- and temperature-sensing neurons. Cells overexpressing the TRPM8 channel can be activated by cold temperatures and by a cooling agent, menthol. Our identification of a cold-sensing TRP channel in a distinct subpopulation of sensory neurons implicates an expanded role for this family of ion channels in somatic sensory detection.

Introduction

The vertebrate sensory nervous system enables fine detection of varied external information. While these senses are popularly categorized into five modalities (taste, smell, hearing, sight, and touch), the sense of touch actually consists of the perception of multiple discrete types of stimuli, including temperature, position, and pressure. Correspondingly, electrophysiologists have long realized that recognition of touch is executed by neurons of restricted specificity, such that painful (or noxious) stimuli can activate neurons of a different class than nonnoxious pressure (Scott, 1992; Hensel, 1981). The molecular characterization of sensory neurons has advanced remarkably in recent years, perhaps most notably with the identification of genes that encode receptor families for smell and taste ligands (Adler et al., 2000; Axel, 1995). And yet, a great deal remains unknown about the molecular pathways that lead to the diversity of neurons that sense "touch" and that enable these neurons to translate mechanical or thermal stimuli into action potentials.

The specialized neurons that detect sensory stimuli reside within the dorsal root ganglia (DRG). There, the neuronal cell bodies are embedded within the vertebral column along the dorsolateral side of the neural tube. The DRG neurons extend long axons to peripheral targets such as skin and visceral organs where they detect chemical, mechanical, and thermal stimuli (Scott, 1992). These sensory modalities can be divided into submodalities according to neuronal specificity. For example, in the case of neurons that convey thermal sensation (so-called thermoreceptors), some DRG fibers detect temperatures between 32°C and 43°C, and their activation is associated with sensing a warm stimulus (Julius and Basbaum, 2001). Other fibers can only be activated at temperatures above 43°C (noxious heat), and still others only respond to subambient temperature.

Despite some knowledge of the physiology of thermoreceptors, very little is known about molecules that are involved in temperature detection in DRG neurons. One such molecule is Vanilloid Receptor 1 (VR1), an ion channel gated by heat (temperatures above 43°C) and expressed in a subset of the nociceptive sensory neurons (Caterina et al., 1997). A close relative, Vanilloid Receptor-Like Protein 1 (VRL1), is activated by very high heat (temperatures above 52°C) and is widely expressed in both neuronal and nonneuronal cells (Caterina et al., 1999). VR1 and VRL1 are members of the TRP family of nonselective cation channels (Clapham et al., 2001). In addition to heat, some TRP channels have been implicated as mechano- and osmosensors in invertebrates (Harteneck et al., 2000; Walker et al., 2000). We were intrigued with the possibility that other members of the TRP family are expressed in mammalian sensory neurons and function as receptors for distinct sensory stimuli. Here, we describe cloning of a mammalian TRP channel that is specifically expressed in a subpopulation of the pain- and temperature-sensing DRG neurons. The functional properties of TRPM8 in a heterologous expression system suggest that it is a nonselective cation channel gated by cold stimuli and menthol, a cooling compound. The channel's properties appear to be very similar to those of a cold- and menthol-activated current described recently in native dorsal root ganglion neurons and proposed to have a role in cold sensing (Reid and Flonta, 2001b).

Results

To identify novel TRP channels, we searched genomic DNA databases by constructing a hidden Markov model (HMM) from the known TRP protein sequences of different mammalian species. With this model, we queried the 6 frame translation of all available human sequences and identified multiple putative exons with similarity to the transmembrane domains 4 and 6 of VR1. We were able to amplify a fragment of the mouse homolog of one TRP channel by RT-PCR from mouse DRG RNA (data not shown). Full-length sequence of this gene was derived from a combination of exon-prediction software, PCR, and RACE amplification from newborn mouse

[4]Correspondence: ardem@scripps.edu

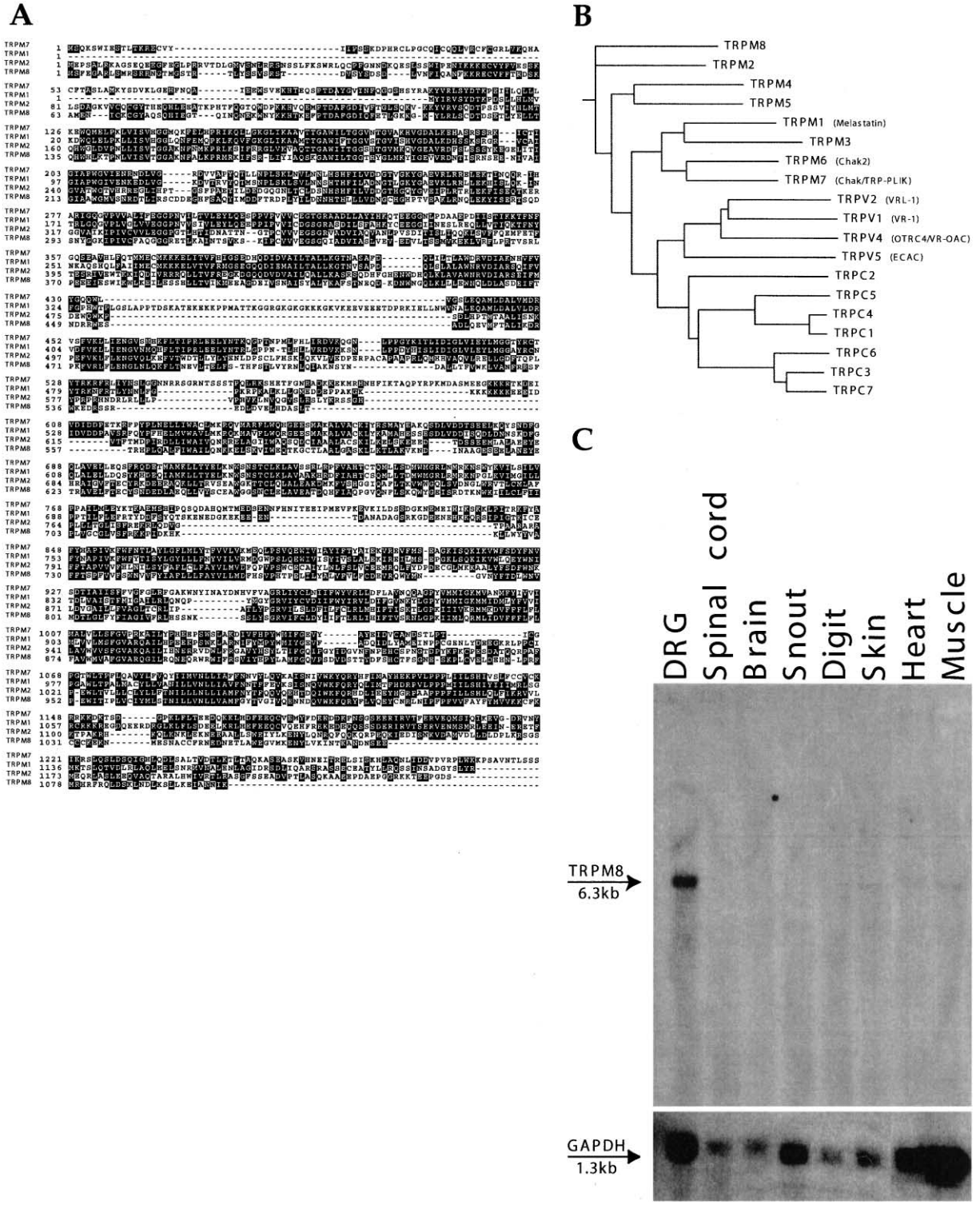

Figure 1. TRPM8 Is a Member of the Melastatin Subfamily of TRP Channels and Is Expressed Predominantly in Dorsal Root Ganglia (DRGs)

(A) Comparison of mouse TRPM8 protein sequence to some of its closest relatives, TRPM1 (human Melastatin, GenBank accession number 6006023), TRPM2 (human, 4507688), and TRPM7 (mouse Chak, 14211382). The alignment was generated using Megalign and Boxshade. Identical or conserved residues are shown in white letters on a black background.

(B) Phylogenetic tree showing protein sequence relationship of different members of the TRP ion channel super-family. TRPs are subdivided into three main subfamilies: TRPMs, TRPVs, and TRPCs. The TRPMs do not contain any ankyrin domains in their N-terminal domains. The transmembrane domains have the highest homology among different classes of TRP channels.

(C) Northern analysis of TRPM8. Northern blot analysis demonstrates that TRPM8 is expressed predominantly in DRGs. The blot was hybridized with ^{32}P-labeled (top) TRPM8 cDNA, then reprobed with GAPDH cDNA (bottom) to control for loading.

DRGs. We have named this protein TRPM8, following the nomenclature suggested in Clapham et al. (2001). Several human ESTs, many of which have been isolated from various cancer tissues, contain fragments of TRPM8 (GenBank accession numbers 8750489, 9149390, 9335992, and 2223353).

Translation of the nucleotide sequence of TRPM8 predicts a protein composed of 1104 amino acid residues (Figure 1A). The overall sequence of mouse TRPM8 is 93% identical to that of the human gene (data not shown). Its closest relative is TRPM2 (42% identity; Figures 1A and 1B). TRPM8 belongs to the "long" or Melastatin subfamily of TRP channels, a group of TRPs characterized by their lack of ankyrin domains in the N terminus. TRP channels are predicted to contain six transmembrane (TM) domains, although at least one is predicted to have seven membrane-spanning domains (Nagamine et al., 1998). A Kyte-Doolittle plot suggested the presence of eight distinct hydrophobic peaks in TRPM8 sequence, which could represent six to eight predicted transmembrane domains (data not shown). Overall, the predicted transmembrane domains are within amino acids 695–1024 of TRPM8. Outside of this region, the only predicted secondary structures are coiled-coil domains present in both the N- and C-terminal portions of the protein (data not shown; Burkhard et al., 2001). Coiled-coil domains are implicated in oligomerization of GABA-B channels and have previously been predicted in some TRP channels (Funayama et al., 1996; Margeta-Mitrovic et al., 2000).

We knew TRPM8 to be expressed in DRGs, since we PCR-cloned the TRPM8 transcript from newborn DRG cDNA. To determine the overall tissue distribution of TRPM8, we used a probe corresponding to nucleotides 1410–1980 of the mouse TRPM8 sequence for Northern blot analysis. No TRPM8 expression was detected using commercial Northern blots (data not shown). We then used blots from newborn and adult mice that included tissues relevant for somatic sensation, including DRG, spinal cord, and different sources of skin (Figure 1C and data not shown). One mRNA species of approximately 6.3 kb was present predominantly in DRGs. Further analysis of TRPM8 expression was performed by in situ hybridization. Digoxygenin-labeled probes showed specific expression in DRG and trigeminal ganglia (cranial sensory neurons innervating the mouth and jaw) in newborn and adult mouse, but not in day 13 embryos (Figures 2A and 2B and data not shown). TRPM8 expression was restricted to approximately 5%–10% of adult DRG neurons. The average size of the neurons positive for TRPM8 was 18 $\pm$ 3.1 μm (mean $\pm$ standard deviation, $n = 69$) and can be classified as small-diameter c fiber-containing neurons, which in mouse are defined as smaller than 25 μm. TRPM8 is not expressed in heavily myelinated neurons marked by Neurofilament (NF) antibodies, which correlates well with TRPM8 expression in small-sized neurons (Figures 2D–2F). TRPM8$^+$ neurons thus appear to belong to a subset of nociceptive or thermoceptive neurons that express trkA, an NGF receptor, during development (Huang and Reichardt, 2001). In the absence of NGF or trkA, DRG neurons that normally express this receptor die through apoptosis during embryonic development (Huang and Reichardt, 2001). To prove that TRPM8 is expressed in trkA-dependent neurons, we evaluated TRPM8 expression in DRGs from newborn trkA null mice. The expression of TRPM8 was completely abolished in the mutant ganglia (Figures 2B and 2C). We have further shown that TRPM8 is not coexpressed with VR1, which marks a class of nociceptors that respond to capsaicin and noxious heat (Figures 2G–2I). This observation is confirmed by the lack of TRPM8 coexpression with either CGRP or IB4, two well-characterized nociceptive antigens that together mark 90% of VR1$^+$ DRG neurons (Figures 2J–2O; Snider and McMahon, 1998; Tominaga et al., 1998). This data strongly suggests that TRPM8 is expressed in a subpopulation of thermoceptive/nociceptive neurons distinct from the well-characterized heat- and pain-sensing neurons marked by VR1, CGRP, or IB4.

Given the similarity of TRPM8 to TRPV family members and its unique expression pattern within the DRG, we tested whether disparate sensory stimuli activate TRPM8. The full-length murine TRPM8 was stably expressed in Chinese hamster ovary (CHO) cells and evaluated for channel properties. We loaded TRPM8-expressing cells with the Ca^{2+} indicator Fura-2 and used conventional microscopy to monitor changes in fluorescence, which reflected changes in the intracellular calcium concentration. CHO cells do not express an endogenous TRPM8 isoform (data not shown) and therefore served as a control along with a cell line stably transfected with a VR1-expressing plasmid. Capsaicin (10 μM), an activator of VR1, did not evoke a response in TRPM8-expressing cells (data not shown). Neither hypoosmotic solutions, known to generate Ca^{2+} responses in TRPV3-expressing cells, nor hypertonic buffer elicited a response in TRPM8-expressing cell lines (data not shown; Liedtke et al., 2000; Strotmann et al., 2000). An increase in temperature (25°C–50°C), a potent stimulus for VR1, also did not alter intracellular calcium levels (data not shown). However, when the temperature was lowered from 25°C to 15°C, an increase in intracellular calcium was observed in TRPM8-expressing cells (Figures 3A and 3B). This response was not observed in nontransfected CHO cells or in the VR1-expressing cell line (Figures 3A and 3B and data not shown). Addition of a 10°C stimulus also evoked an influx of Ca^{2+} (data not shown). This response was dependent on Ca^{2+} in the buffer, because removal of extracellular calcium suppressed the temperature response (Figure 3B). The dependence on outside calcium is indicative of a cation-permeable channel localized at the plasma membrane. A potent blocker of the heat response for VR1, ruthenium red (at 5 μM), did not suppress the temperature response (data not shown).

Since TRPM8 responded to a decrease in temperature, we performed additional experiments to investigate the temperature threshold at which intracellular calcium ($[Ca^{2+}]_i$) begins to rise in TRPM8-expressing cells. Cells were incubated at 35°C (normal skin temperature) for several minutes, followed by a decrease in temperature to 13°C (Figure 3C). The temperature response in mouse TRPM8-CHO cells showed a threshold of 22°C–25°C at which $[Ca^{2+}]_i$ started to increase, followed by a marked increase when the temperature of the buffer reached ~15°C. These experiments indicate that at physiologically relevant temperatures, the upper activation threshold for TRPM8 is ~23°C.

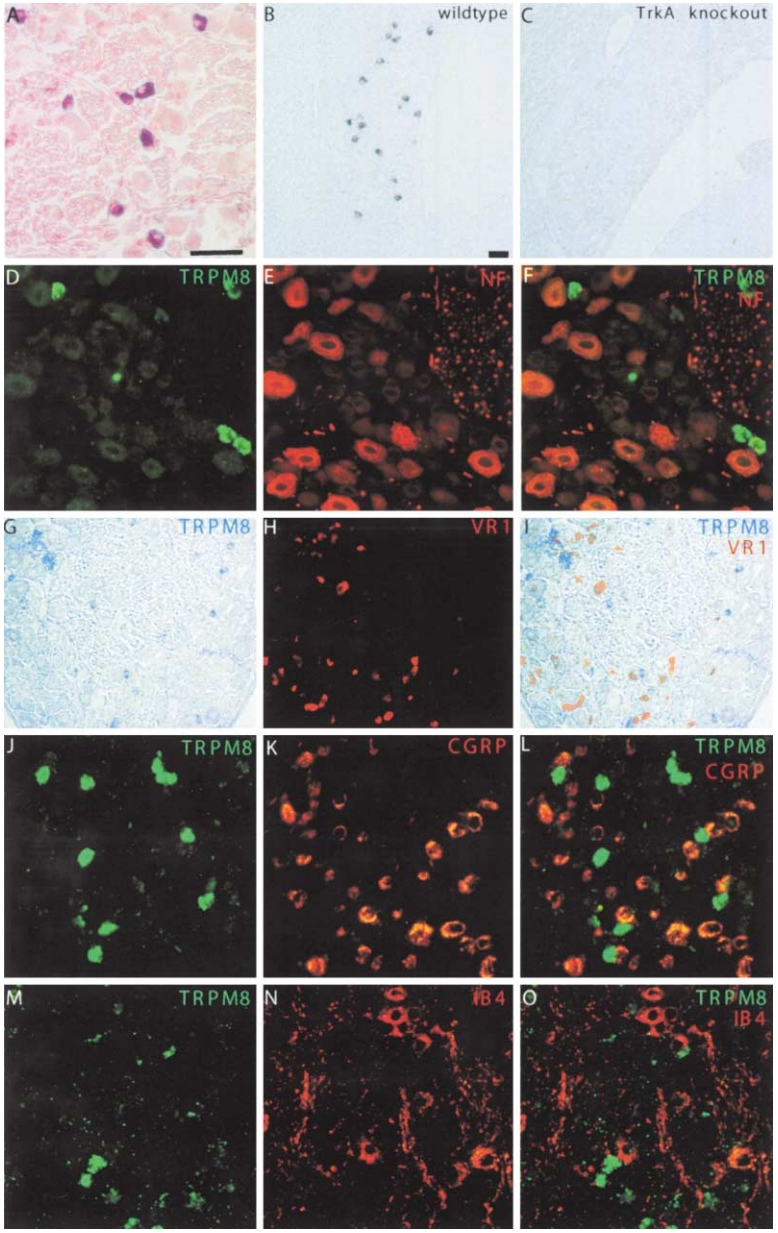

Figure 2. In Situ Hybridization Analysis of TRPM8

(A) Digoxygenin in situ hybridization (purple) showing expression of TRPM8 in small neurons of the trigeminal ganglia of adult mice. The bar is 50 μm in (A), (D)–(F), and (J)–(O).

(B and C) TRPM8 mRNA is present in newborn wild-type DRGs but not in trkA mutants. The bar is 50 μm in (B), (C), and (G)–(I).

(D–F) TRPM8 is not expressed in heavily myelinated neurons labeled by Neurofilament (NF150) antibody. Double-staining of TRPM8 (mRNA) and NF150 antibody in adult mouse DRGs do not show coexpression.

(G–I) TRPM8 mRNA is not present in adult DRG neurons labeled with a VR1 antibody.

(J–L) Double-staining with TRPM8 (mRNA) and CGRP antibody or IB4 binding (M–O) in adult mouse DRGs demonstrate a mutually exclusive expression pattern.

Menthol, a compound commonly used for its cooling properties, was tested as a stimulus on TRPM8-expressing CHO cells. Nontransfected CHO cells were completely insensitive to menthol (tested up to 1 mM; Figures 4A and 4B). However, upon treatment of TRPM8 cells (incubated at 25°C), intracellular fluorescence increased significantly within seconds in response to menthol concentrations of 10 μM and 100 μM (Figures 4A and 4B). Additionally, as with the temperature stimulus, depletion of calcium from the extracellular buffer suppressed the calcium response (Figures 4A and 4B). We next tested the effect menthol had at different temperatures. Incubation of TRPM8-expressing cells at 33°C revealed that 10 μM menthol did not induce a calcium response as observed at 25°C, but upon lowering the temperature to 30°C, intracellular calcium levels increased (Figure 4C). Menthol thus appears to mimic the effect of lowering the temperature on TRPM8-expressing cells.

To investigate the membrane responses to cold and menthol, we carried out voltage clamp experiments on TRPM8-expressing cells. Temperature ramps from 35°C to 7°C–13°C evoked inward currents at a holding potential of −60 mV and outward currents at +40 or +60 mV. Currents increased in amplitude as the temperature was lowered and usually showed some degree of desensitization at the coldest temperatures tested (<10°C; Figure 5A). The temperature threshold for current activation showed no dependence on membrane potential, and individual cells activated at temperatures between 19°C and 25°C, with a mean threshold of 21.79°C ± 0.64°C (n = 5). Analysis of the current-voltage relationships of the response to a cold stimulus with CsCl-filled recording pipettes and a typical NaCl-based external solution revealed an outwardly rectifying current with a reversal potential (E_{rev}) close to 0 mV, which is typical of a nonselective cation channel (Figure 5B).

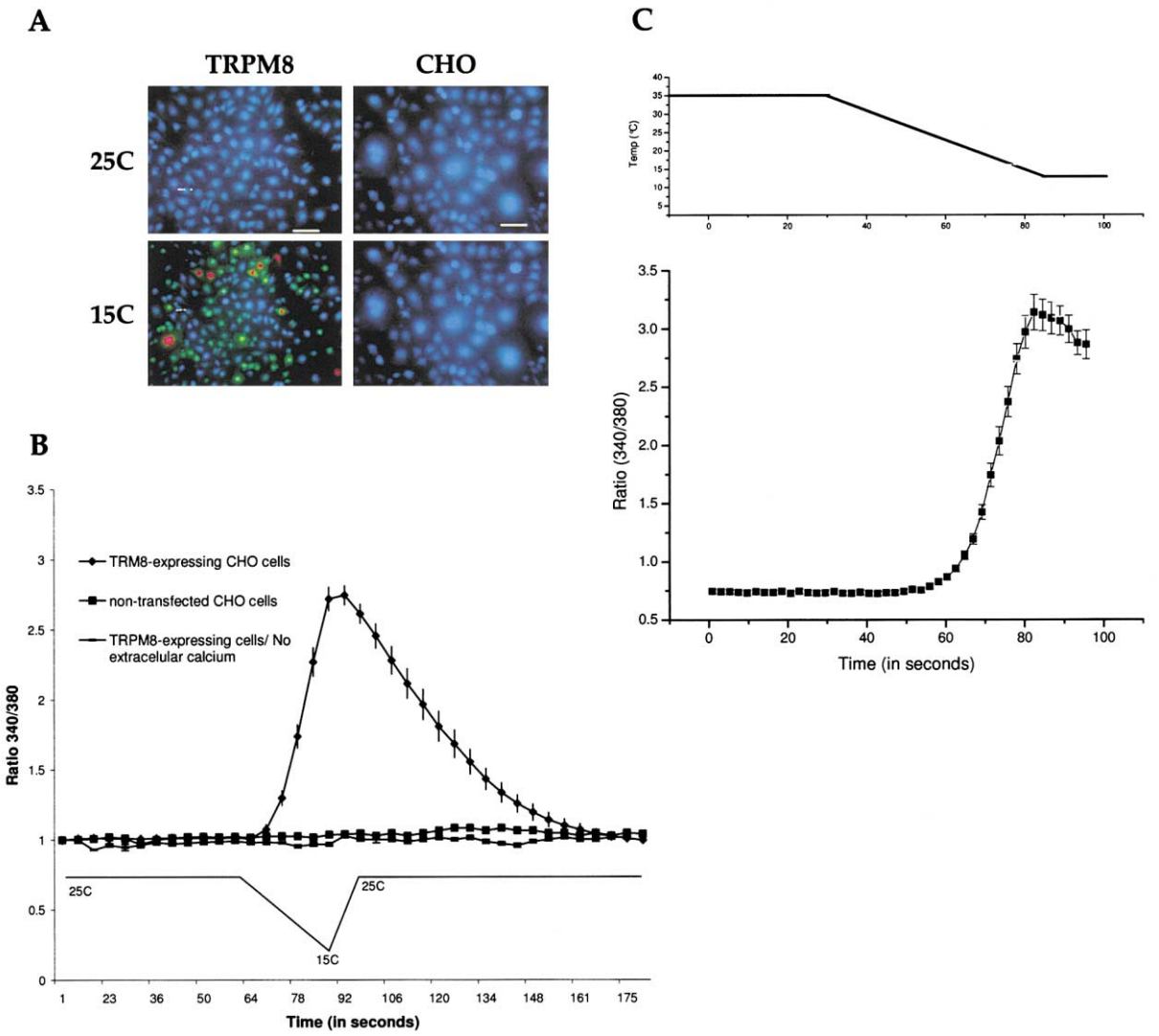

Figure 3. Increase in Intracellular Calcium $[Ca^{2+}]_i$ Concentration in TRPM8-Expressing CHO Cells in Response to Cold

(A) Representative images taken from calcium imaging experiments. TRPM8 stably transfected CHO cells and nontransfected CHO cells loaded with Fura-2 and viewed with fluorescence microscopy. Upon addition of a 15°C cold stimulus (measured in the cell chamber by a miniature thermocouple), an increase in fluorescence is observed as the buffer in the cell chamber is cooled, indicative of an increase in intracellular Ca^{2+} in TRPM8-expressing cells. Increasing levels of intracellular Ca^{2+} are indicated by a change in color (blue-green-yellow-red). The highest levels of $[Ca^{2+}]_i$ are indicated in red. The same microscopic field of cells is shown before and after the cold stimulus. The bars indicate 50 μm.

(B) TRPM8-transfected CHO cells show a rapid increase in $[Ca^{2+}]_i$ when the temperature is lowered from 25°C to ~15°C. The stimulus period is indicated below the traces. Nontransfected CHO cells do not show a response to cold. Removal of external Ca^{2+} completely suppressed the response to cooling. Experiments were performed in triplicate. The average response (±SEM) of 20–30 cells from a representative experiment is presented.

(C) Increase in $[Ca^{2+}]_i$ due to decrease in temperature from 35°C to 13°C in $TRPM8^+$ cells. The panel shows mean ± SEM for 34 individual cells. Note the increase started to occur between 22°C and 25°C.

Application of menthol-evoked rapidly activating currents in TRPM8-expressing cells, but not in nontransfected CHO cells, at temperatures above the threshold for cold activation (>23°C; Figure 6A). The menthol-activated current showed pronounced outward rectification (Figure 6B) with an E_{rev} of -9.28 ± 0.75 mV ($n = 12$) that is similar to the E_{rev} for the cold-activated current under the same ionic conditions. These currents could be inactivated by raising the temperature (Figure 6A), suggesting that menthol shifts the threshold for activation to higher temperatures, which agrees with our calcium imaging experiments. To test this idea further, we obtained concentration-response curves for menthol-evoked currents at two temperatures (22°C and 35°C), using positive membrane potentials to increase the size of the currents (Figures 7A and 7B). The concentration-response relationship was shifted to the left at the lower temperature with a marked increase in the maximum amplitudes (Figures 7A and 7B). We next used changes in E_{rev} to determine the ion selectivity of the menthol-

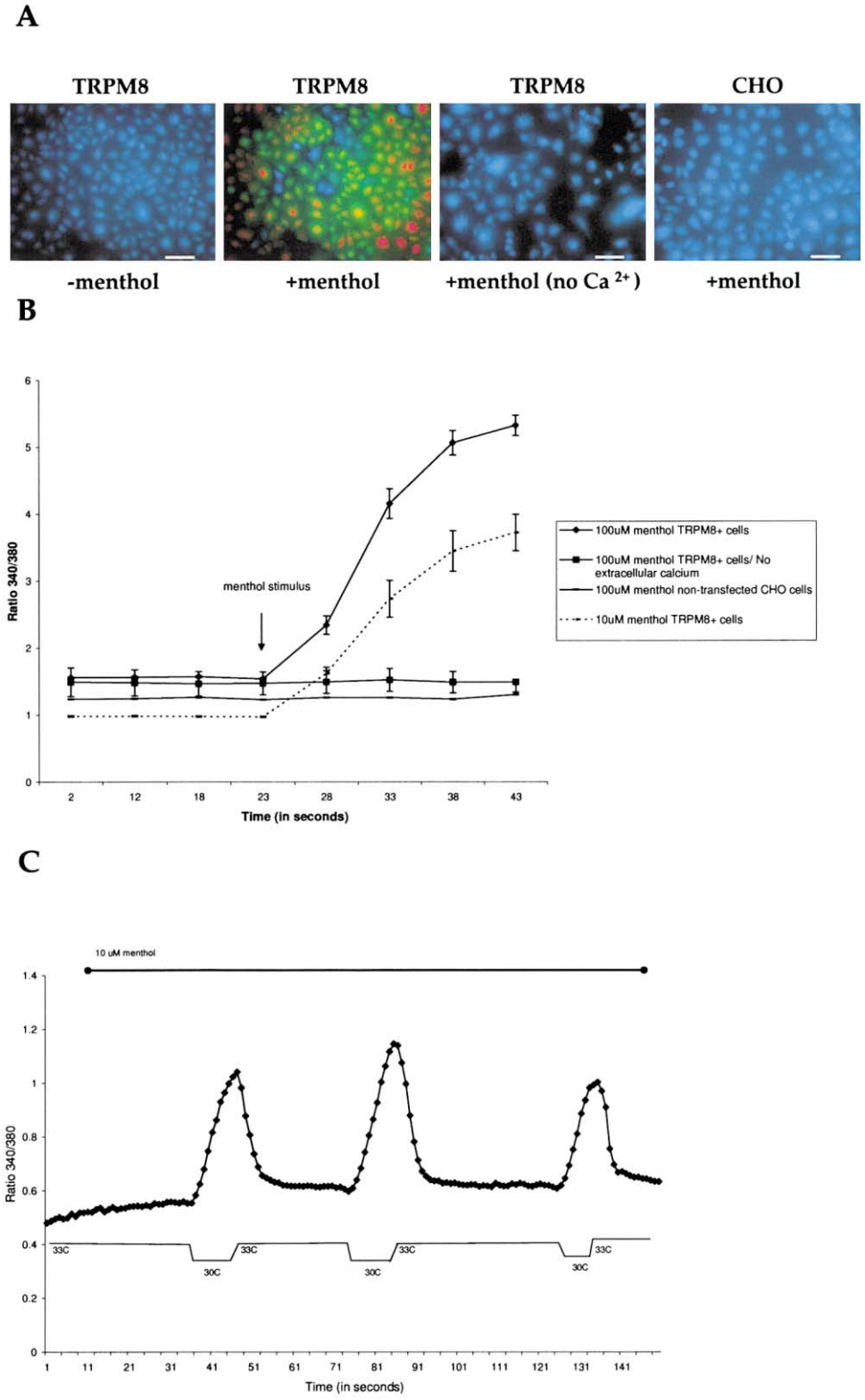

Figure 4. Increase in Intracellular Calcium $[Ca^{2+}]_i$ Concentration in TRPM8-Expressing CHO Cells in Response to Menthol

(A) Individual TRPM8$^+$ cells respond to menthol at 25°C. Representative images from calcium imaging experiments illustrate a large influx of calcium in response to a menthol stimulus (100 μM). This response was not seen in nontransfected CHO cells or without extracellular calcium. Intracellular calcium concentration is indicated by colors described in Figure 3A. The same field of cells is shown for TRPM8 before and after menthol treatment (with calcium). The other images presented were taken immediately after the menthol stimulus.

(B) TRPM8 responds to menthol at 25°C. Intensity of the TRPM8 response is dependent on menthol concentrations. A 10-fold increase in

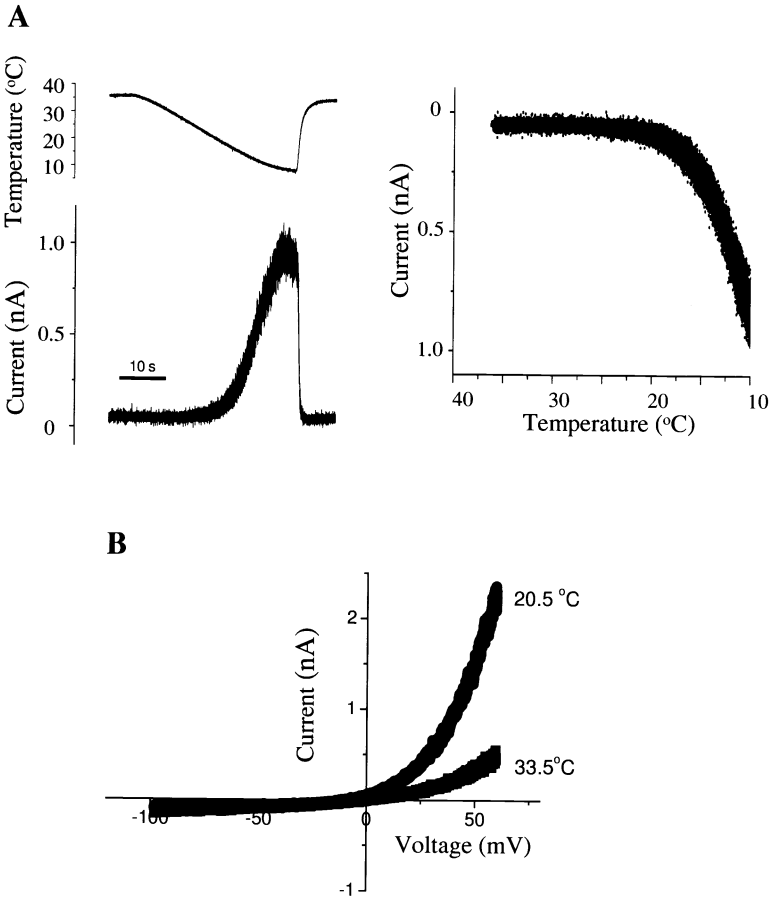

Figure 5. Current Evoked by Reduction in Temperature in TRPM8-Expressing CHO Cells

(A) Outward currents evoked at +60 mV by reducing the temperature from 35°C to 10°C. In this cell the current activated at 19.3°C as indicated in the right graph.

(B) Current-voltage relationship for currents activated at 20.5°C and 33.5°C. Increasing the temperature reduces the amplitude of outward currents.

activated current. Isotonic replacement of the NaCl in the solution with KCl or CsCl caused small positive shifts in E_{rev}, indicating that the TRPM8 channel discriminated poorly between these cations (data not shown). From the changes in E_{rev} measured on individual cells (external NaCl to KCl gave a shift of $+7.38 \pm 1.43$ mV, $n = 7$; NaCl to CsCl gave a shift of $+9.09 \pm 0.36$ mV, $n = 5$), we calculated a permeability sequence of $Cs > K > Na$ with $P_{Cs}/P_{Na} = 1.43$ and $P_K/P_{Na} = 1.34$. Relative calcium permeability was calculated from the E_{rev} values measured with different external calcium concentrations. Increasing the external calcium from 1 to 30 mM, in the absence of external Mg^{2+} ions, shifted E_{rev} by $+11.67 \pm 1.20$ mV, which corresponds to $P_{Ca}/P_{Na} = 0.97$ (data not shown). Thus, TRPM8 is permeable to the monovalent cations, Na, K, and Cs, as well as the divalent cation calcium.

Discussion

The study of temperature perception has recently moved into the molecular arena with the cloning and characterization of the vanilloid receptors. These molecules, members of the TRP family of membrane channels, are activated by high temperatures to mediate a cation influx (Clapham et al., 2001). Here, we show that another relative, TRPM8, is instead activated by cold stimuli. We have furthermore found that TRPM8 is expressed in a very select group of dorsal root ganglia (DRG) neurons that share characteristics of thermoreceptive neurons.

Ambient skin temperature is maintained near 32°C. Temperatures above this point activate neurons within the dorsal root ganglia (DRG) and lead to the perception of warmth and, beyond 43°C–45°C, noxious pain. VR1, a heat-gated TRP channel, is involved in detecting noxious heat stimuli and is found in DRG neurons (Julius and Basbaum, 2001). At temperatures below ambient, another set of DRG neurons is activated. Although an exact threshold for cold pain has not been found, it is thought that a separate set of neurons is responsible for innocuous cool temperatures (20°C–30°C) and for painful cold. A further division of specialization seems to exist between neurons that are activated by cold

menthol concentration resulted in a larger influx of Ca^{2+}. This response was suppressed in the absence of Ca^{2+}. Nontransfected CHO cells exhibited no increase in $[Ca^{2+}]i$ upon application of menthol. Experiments were performed in triplicate. The average response (±SEM) of 20–30 cells from a representative experiment is presented.

(C) At 33°C, 10 μM menthol does not elicit an influx of Ca^{2+}. When the temperature of the bath solution is lowered to 30°C, a marked increase in intracellular Ca^{2+} is observed. These experiments suggest that menthol simulates the effect of cooling in TRPM8-expressing cells.

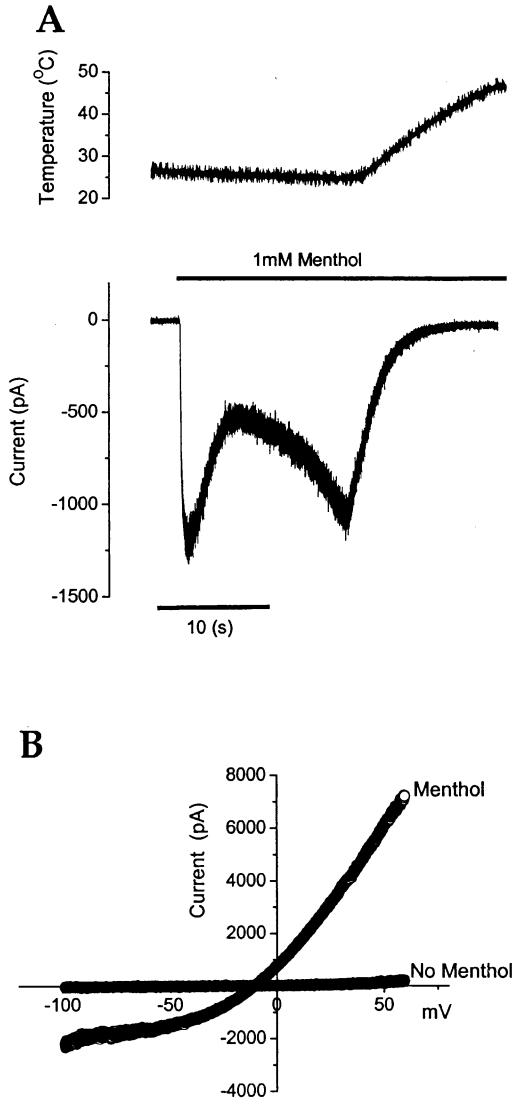

Figure 6. Current Evoked by Menthol in TRPM8-Expressing CHO Cells

(A) Inward currents evoked by 1 mM menthol (V_h = −60 mV) are inactivated by increasing the temperature from 25°C to 45°C.

(B) Current-voltage relationship for response to 1 mM menthol. Currents show pronounced outward rectification in the presence of menthol not seen in the absence of this agonist.

temperatures (4°C–15°C) and temperatures below 0°C (Simone and Kajander, 1997). The downstream events comprising the cold-stimulated response are also not clear. It has been suggested that cold may depolarize nerve fibers by inhibiting a sodium-potassium ATPase or by inhibiting a potassium channel, and recent studies proposed that cold stimulates calcium influx into cells (Reid and Flonta, 2001a, 2001b; Suto and Gotoh, 1999).

We have discovered that cells overexpressing TRPM8 show increased intracellular calcium levels when subjected to cold temperatures ranging from 23°C to 10°C (the lower limit of our temperature-controlled perfusion system). The calcium influx and electrophysiological studies demonstrate that TRMP8 is a nonselective plasma membrane cation channel activated by cold temperatures. The ionic permeability of TRPM8 is similar to that of other TRP channels, which are permeable to both monovalent and divalent cations, although calcium permeability estimates (P_{Ca}/P_{Na}) vary from 0.3 to 14 (see for example Harteneck et al., 2000). Menthol is a cooling compound that likely acts on endogenous cold-sensitive channel(s) (Schafer et al., 1986). Our observation that TRPM8-expressing cells are activated and modulated by menthol reinforces the idea that TRPM8 indeed functions as a cold-sensitive channel in vivo. The finding that the sensitivity to menthol is dependent on temperature is consistent with the behavior of a subset of isolated DRG neurons that show a raised "cold" threshold in the presence of menthol (Reid and Flonta, 2001b). The mechanism of TRPM8 activation by cold is not yet known: TRPM8 could be directly gated by cold stimulus through a conformational change, or cold temperatures could act through a second messenger system that in turn activates TRPM8. Our experiments do not distinguish between these possibilities, although the rapid activation by menthol would suggest a direct gating mechanism, at least for this mode of activation.

The expression pattern we have documented for TRPM8 is consistent with a role in cold thermoception. First, we have found TRPM8 mRNA to be highly specific to DRG neurons, as might be expected. Within the DRG, TRPM8 is expressed in the small-diameter nonmyelinated neurons, which correspond to the c fiber thermoreceptor and nociceptors (Scott, 1992). The lack of TRPM8 expression in trkA knockout mice, whose DRGs lack all thermoreceptor and nociceptive neurons, corroborates this finding. Futhermore, the lack of coexpression with VR1, CGRP, or IB4 in the adult suggests that TRPM8 is expressed in a unique population of DRG neurons distinct from well-characterized heat nociceptors. Both soma size of neurons that express VRL-1 (medium-large neurons) and their coexpression with NF200 (80% coexpression; Caterina et al., 1999) strongly argues that cells expressing TRPM8 and VRL-1 are also distinct. Therefore, by using various markers we have shown that TRPM8 is expressed in a subclass of nociceptors/thermoreceptors that is distinct from noxious heat-sensing neurons, and this correlates well with physiological studies of cold-sensitive DRG neurons (Hensel, 1981). As such, TRPM8 will be an important starting point for molecular studies of cold perception. A human gene with a high degree of similarity to mouse TRPM8 but no known function was recently shown to be expressed in prostate tissue (Tsavaler et al., 2001).

All three molecules identified as thermoreceptors belong to the TRP group of channels. VR1 and VRL1 are closely related (47% identity) and sense heat, while TRPM8 (which is 21% identical to VR1) responds to cold temperature. The most significant similarity between TRPM8 and TRPVs is found in the transmembrane domain, while the intracellular N and C termini are quite divergent. All three, however, act as calcium-permeable nonselective cation channels. Further work on the relationship between structure and function of these channels may reveal much about how thermal energy is transmitted into neural activity. Given that humans can detect temperature variations as small as 1°C, it is likely that other channels and receptors are involved in tempera-

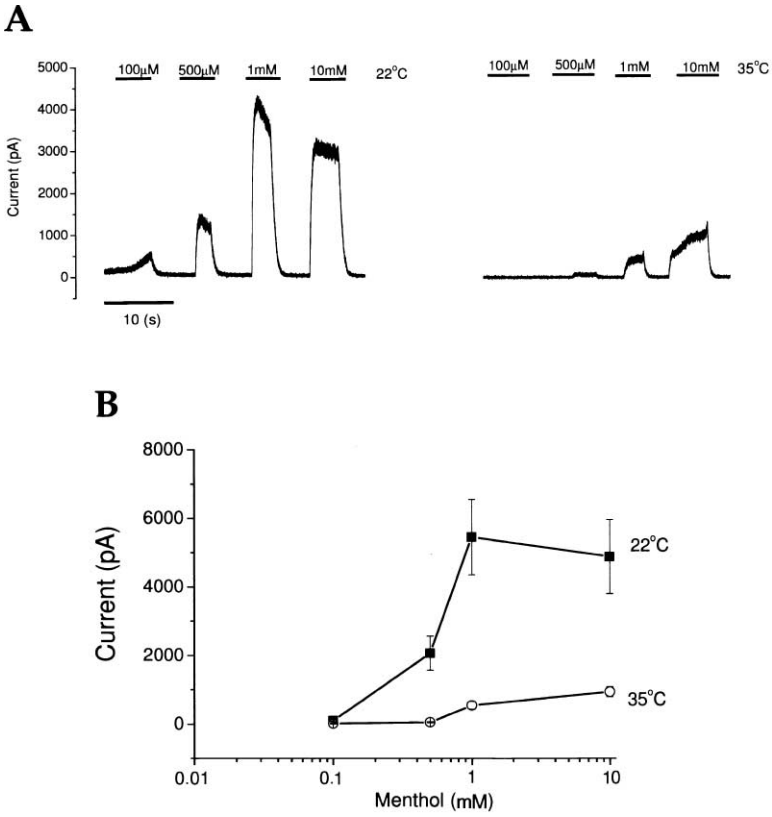

Figure 7. Current Evoked by Menthol at +60 mV

(A) Single examples, from two different cells, of current evoked by applying 0.1, 0.5, 1, and 10 mM menthol at 22°C and 35°C.

(B) Comparison of response (mean ± SEM, n = 5 for all points) of current evoked by menthol either at 22°C or 35°C.

ture perception. For example, although DEG/EnaC channels do not respond to thermal stimuli alone, their activity can be modulated by cold temperature (Askwith et al., 2001). As the first molecule to respond to cold temperatures and menthol, TRPM8 offers interesting insight into the fundamental biology of cold perception. Modulation of TRPM8 activity may also be relevant for therapeutic applications: cold treatment is often used as a method of pain relief, and in some instances, hypersensitivity to cold can lead to cold allodynia in patients suffering from neuropathic pain.

Experimental Procedures

Molecular Cloning of mTRPM8

For PCR cloning, primer 163f (5′-CAAGTTTGTCCGCCTCTTTC) and 164r (5′-AACTGTCTGGAGCTGGCAGT) were designed from the HMM sequences for TRPM8 as a result of blast hits and used to amplify a 699 nucleotide fragment of TRPM8 from newborn DRG cDNA. From this initial sequence and exon prediction programs, rapid amplification of cDNA ends (RACE) PCR (Clontech) was used to obtain the 5′ and 3′ ends of TRPM-8 from mouse newborn DRG cDNA following the manufacturer's protocol.

Expression Analysis

Northern blots were made as follows: total RNA was purified from mouse newborn and adult tissues using TRIzol LS (Invitrogen/GIBCO Life Technologies), followed by poly(A)$^+$ purification with Oligotex (Qiagen) according to the manufacturer's protocols. Approximately 3 μg of sample was electrophoresed on 1% glyoxal gels, transferred, and hybridized at high stringency with a ^{32}P-labeled probe representing nucleotides 1410–1980 of the mouse full-length TRPM8 sequence. Commercial Northern blots (Clontech) were hybridized with the same TRPM8 probe. Blots were hybridized for 3 hr at 68°C in ExpressHyb hybridization solution (Clontech), washed according to the manufacturer's high-stringency washing protocol, and exposed to a phosphoimager screen for 1–3 days.

For in situ hybridizations, newborn and adult tissues were dissected, fixed in 4% paraformaldehyde in PBS, cryoprotected, and frozen in liquid nitrogen in OCT mounting medium. Cryostat sections (10 μm) were processed and hybridized with a digoxygenin cRNA probe generated by in vitro transcription (Roche Biochemicals). The mouse TRPM8 mRNA specific antisense riboprobe corresponded to nucelotides 1410–1980 of the mTRPM8 sequence. Fluorescence detection and double-labeling experiments were carried out with the tyramide signal amplification kit (TSA; NEN) essentially as previously described (Dong et al., 2001). Following in situ hybridization, immunofluorescence was performed with anti-CGRP (1:100; Biogenesis), IB-4 (10 μg/ml; Sigma), anti-VR1 (1/2000; Abcam), and anti-NF150 (1/1000; Chemicon) and was detected with FITC or CY3 (10 μg/ml; Jackson Immunoresearch). Although all panels shown in these studies demonstrate lack of coexpression, this was not due to technical issues since additional probes/antibodies were used as controls to ensure our double-labeling protocol with the TRPM8 in situ probe was working (data not shown).

Generation of Mouse TRPM8-Expressing CHO Cell Lines

Mouse TRPM8 cDNA was subcloned in pcDNA5 (Invitrogen) and transfected into CHO-K1/FRT cells using Fugene 6 (Roche). The transfected cells were selected by growth in MEM medium containing 200 μg/ml hygromycin (GIBCO-BRL). Populations were frozen at early passage numbers, and these stocks were used for further studies. Stable clones that expressed the mRNAs were identified by Northern blot analysis as well as Southern blotting to confirm integration site (not shown).

Imaging of Intracellular Calcium Levels $[Ca^{2+}]_i$

Calcium imaging experiments were performed essentially as previously described (Savidge et al., 2001). Briefly, cells were plated on glass coverslips, loaded with Fura-2 acetoxymethyl ester (2.5–5

mM), and incubated for 30–60 min at room temperature in 1.5 mM of pluronic acid (Molecular Probes, Eugene, OR) in a HEPES-buffered saline (2 mM Ca^{2+}). Coverslips were placed in a laminar flow perfusion chamber (Warner Instrument Corp.) and constantly perfused with HEPES-buffered saline (2 mM Ca^{2+}) via a local perfusion pipette through which buffer and chilled solutions were also applied. Chilled stimulations consisted of a linear decrease ($\sim$1–1.5°C s^{-1}) in perfusate temperature from 33°C to 10°C. Perfusate temperature was controlled by a regulated Peltier device and was monitored in the cell chamber by a miniature thermocouple. Alternatively, cells were plated on 24-well tissue culture plates and loaded with Fura-2, and application of solutions was performed with a 3 cc syringe over a period of 10 s. Images of Fura-2-loaded cells with the excitation wavelength alternating between 340 nm and 380 nm were captured with a cooled CCD camera. Following subtraction of background fluorescence, the ratio of fluorescence intensity at the two wavelengths was calculated. Ratio levels in groups of 20–40 individual cells were analyzed using MetaFluor (Universal Imaging Corporation). All graphs are averaged responses from groups of 20–30 individual cells from representative single experiments. All experiments have been repeated on three separate occasions, and similar results were obtained. Hanks balanced salt solution (HBSS), phosphate buffered saline (PBS), and all cell culture reagents were obtained from GIBCO-BRL. Ruthenium red, capsaicin, and menthol were obtained from Sigma.

Electrophysiology

Cells were plated onto poly-D-lysine-coated coverslips for recording purposes, and recordings were undertaken 18–24 hr later. Experiments were carried out at room temperature using whole-cell voltage clamp technique, with an Axopatch 2B amplifier filtered at 5 kHz and pClamp suite of software (Axon Instruments). Series-resistant compensation was 80% for all experiments, using 2–5 M Ω fire-polished pipettes. Recording solutions were as follows: pipette solution for all experiments was (mM) CsCl, 140; $CaCl_2$, 1; EGTA, 10; HEPES, 10; MgATP, 2; titrated to pH 7.4 with CsOH. For menthol- and cold-activated currents, the bath solution was [(mM): NaCl, 140; KCl, 5; Glucose; 10, HEPES, 10; $CaCl_2$, 2; $MgCl_2$, 1; titrated to pH 7.4 with NaOH]. Current-voltage relationships were used to evaluate reversal potentials with voltage ramps from –100 to +60 mV (2 s duration). For the permeability studies for the monovalent ions, the NaCl in a simplified bath solution [(mM): NaCl, 140; Glucose; 10, HEPES, 10; $CaCl_2$, 2; $MgCl_2$, 1] was substituted by either equimolar CsCl or KCl (titrated with CsOH or KOH). For calcium permeability estimates, the bath solutions contained (mM) NaCl, 100; Glucose, 10; and Hepes, 10 (titrated with NaOH), plus 1 or 30 mM $CaCl_2$. Osmolarity of solutions was adjusted by addition of sucrose. Permeability ratios for the monovalent cations to Na (P_X/P_{Na}) were calculated as follows: $P_X/P_{Na} = E_{shift} = \{RT/F\} \log (P_X/P_{Na}[X]_O / [Na]_O)$, where F is Faraday's constant, R is the universal gas constant, and T is absolute temperature. For measurements of calcium permeability, P_{Ca}/P_{Na} was calculated as follows: $E_{shift} = \{RT/F\} \log \{[Na]_O + 4B'[Ca]_{O\,(2)}\}/\{ [Na]_O 4B'[Ca]_{O\,(1)}\}$, where $B' = P'_{Ca}/P_{Na}$ and $P'_{Ca} = P_{Ca}/(1 + e^{EF/RT})$ and $[Ca]_{O\,(1)}$ and $[Ca]_{O\,(2)}$ refer to the two different calcium concentrations. Local perfusion of menthol was via a TC^2 bip temperature controller; a Marlow temperature controller was used for the cooling ramps.

Acknowledgments

The authors would like to thank Carey Backus, Keith Ching, Todd Hricic, Elizabeth Gardiner, James Mainquist, James Watson, and A.J. Wilson for technical help and John Hogenesch, Nancy Hong, Steve Kay, Lou Reichardt, and Pete Schultz for valuable advice. This work was partially supported by a grant from Novartis. A.P. is a Basil O'Connor Scholar.

Received: January 25, 2002
Revised: February 7, 2002
Published online: February 11, 2002

References

Adler, E., Hoon, M.A., Mueller, K.L., Chandrashekar, J., Ryba, N.J., and Zuker, C.S. (2000). A novel family of mammalian taste receptors. Cell *100*, 693–702.

Askwith, C.C., Benson, C.J., Welsh, M.J., and Snyder, P.M. (2001). DEG/ENaC ion channels involved in sensory transduction are modulated by cold temperature. Proc. Natl. Acad. Sci. USA *98*, 6459–6463.

Axel, R. (1995). The molecular logic of smell. Sci. Am. *273*, 154–159.

Burkhard, P., Stetefeld, J., and Strelkov, S.V. (2001). Coiled coils: a highly versatile protein folding motif. Trends Cell Biol. *11*, 82–88.

Caterina, M.J., Schumacher, M.A., Tominaga, M., Rosen, T.A., Levine, J.D., and Julius, D. (1997). The capsaicin receptor: a heat-activated ion channel in the pain pathway. Nature *389*, 816–824.

Caterina, M.J., Rosen, T.A., Tominaga, M., Brake, A.J., and Julius, D. (1999). A capsaicin-receptor homologue with a high threshold for noxious heat. Nature *398*, 436–441.

Clapham, D.E., Runnels, L.W., and Strubing, C. (2001). The TRP ion channel family. Nat. Rev. Neurosci. *2*, 387–396.

Dong, X., Han, S., Zylka, M.J., Simon, M.I., and Anderson, D.J. (2001). A diverse family of GPCRs expressed in specific subsets of nociceptive sensory neurons. Cell *106*, 619–632.

Funayama, M., Goto, K., and Kondo, H. (1996). Cloning and expression localization of cDNA for rat homolog of TRP protein, a possible store-operated calcium (Ca^{2+}) channel. Brain Res. Mol. Brain Res. *43*, 259–266.

Harteneck, C., Plant, T.D., and Schultz, G. (2000). From worm to man: three subfamilies of TRP channels. Trends Neurosci. *23*, 159–166.

Hensel, H. (1981). Thermoreception and Temperature Regulation (London: Academic Press).

Huang, E.J., and Reichardt, L.F. (2001). Neurotrophins: roles in neuronal development and function. Annu. Rev. Neurosci. *24*, 677–736.

Julius, D., and Basbaum, A.I. (2001). Molecular mechanisms of nociception. Nature *413*, 203–210.

Liedtke, W., Choe, Y., Marti-Renom, M.A., Bell, A.M., Denis, C.S., Sali, A., Hudspeth, A.J., Friedman, J.M., and Heller, S. (2000). Vanilloid receptor-related osmotically activated channel (VR-OAC), a candidate vertebrate osmoreceptor. Cell *103*, 525–535.

Margeta-Mitrovic, M., Jan, Y.N., and Jan, L.Y. (2000). A trafficking checkpoint controls GABA(B) receptor heterodimerization. Neuron *27*, 97–106.

Nagamine, K., Kudoh, J., Minoshima, S., Kawasaki, K., Asakawa, S., Ito, F., and Shimizu, N. (1998). Molecular cloning of a novel putative Ca^{2+} channel protein (TRPC7) highly expressed in brain. Genomics *54*, 124–131.

Reid, G., and Flonta, M. (2001a). Cold transduction by inhibition of a background potassium conductance in rat primary sensory neurones. Neurosci. Lett. *297*, 171–174.

Reid, G., and Flonta, M.L. (2001b). Physiology. Cold current in thermoreceptive neurons. Nature *413*, 480.

Savidge, J.R., Ranasinghe, S.P., and Rang, H.P. (2001). Comparison of intracellular calcium signals evoked by heat and capsaicin in cultured rat dorsal root ganglion neurons and in a cell line expressing the rat vanilloid receptor, VR1. Neuroscience *102*, 177–184.

Schafer, K., Braun, H.A., and Isenberg, C. (1986). Effect of menthol on cold receptor activity. Analysis of receptor processes. J. Gen. Physiol. *88*, 757–776.

Scott, S.A. (1992). Sensory Neurons: Diversity, Development, and Plasticity (New York: Oxford University Press).

Simone, D.A., and Kajander, K.C. (1997). Responses of cutaneous A-fiber nociceptors to noxious cold. J. Neurophysiol. *77*, 2049–2060.

Snider, W.D., and McMahon, S.B. (1998). Tackling pain at the source: new ideas about nociceptors. Neuron *20*, 629–632.

Strotmann, R., Harteneck, C., Nunnenmacher, K., Schultz, G., and Plant, T.D. (2000). OTRPC4, a nonselective cation channel that confers sensitivity to extracellular osmolarity. Nat. Cell Biol. *2*, 695–702.

Suto, K., and Gotoh, H. (1999). Calcium signaling in cold cells studied

in cultured dorsal root ganglion neurons. Neuroscience *92*, 1131–1135.

Tominaga, M., Caterina, M.J., Malmberg, A.B., Rosen, T.A., Gilbert, H., Skinner, K., Raumann, B.E., Basbaum, A.I., and Julius, D. (1998). The cloned capsaicin receptor integrates multiple pain-producing stimuli. Neuron *21*, 531–543.

Tsavaler, L., Shapero, M.H., Morkowski, S., and Laus, R. (2001). Trp-p8, a novel prostate-specific gene, is up-regulated in prostate cancer and other malignancies and shares high homology with transient receptor potential calcium channel proteins. Cancer Res. *61*, 3760–3769.

Walker, R.G., Willingham, A.T., and Zuker, C.S. (2000). A *Drosophila* mechanosensory transduction channel. Science *287*, 2229–2234.

Accession Numbers

The GenBank accession number of TRPM8 is AF481480.